Biology of Reproduction, 2020, 103(3), 620–629
doi:10.1093/biolre/ioaa100
Research Article
Advance Access Publication Date: 8 June 2020

OXFORD

Research Article

IRX3 and IRX5 collaborate during ovary development and follicle formation to establish responsive granulosa cells in the adult mouse†

Anqi Fu[1], Megan L. Koth[1], Ryan M. Brown[1], Sarah A. Shaw[1], Linda Wang[1], Kathleen J. Krentz[2], Xiaoyun Zhang[3], Chi-chung Hui[3] and Joan S. Jorgensen[1,*]

[1]Department of Comparative Biosciences, School of Veterinary Medicine, University of Wisconsin–Madison, Madison, WI, USA, [2]Genome Editing and Animal Models Core, Biotechnology Center, University of Wisconsin–Madison, Madison, WI, USA and [3]Program in Developmental and Stem Cell Biology, The Hospital for Sick Children and Department of Molecular Genetics, University of Toronto, Toronto, Ontario, Canada

***Correspondence**: University of Wisconsin, School of Veterinary Medicine, 2015 Linden Dr., Madison, WI 53706, USA. Tel: 1-608-890-2337; E-mail: joan.jorgensen@wisc.edu

†**Grant Support:** This work was supported by Canadian Institute of Health Research Operating Grant (CCH), University of Wisconsin Carbone Cancer Center Support Grant, National Institute of Health, National Cancer Institute P30 CA014520 (KJK, JSJ), National Institute of Health, The Eunice Kennedy Shriver National Institute of Child Health and Human Development R01HD075079 (JSJ), Endocrinology and Reproductive Physiology Training Grant, and National Institutes of Health (NICHD) T32HD41921 (AF Trainee).

‡**Conference Presentation:** Presented in part at Fu et al., Oral presentation for ENDO 2019, New Orleans, LA; Fu et al., Oral presentation for the Eighth International Symposium on the Biology of Sex Determination, Kona, Hawaii.

Received 12 February 2020; Revised 27 May 2020; Editorial Decision 1 June 2020; Accepted 5 June 2020

Abstract

Healthy development of ovarian follicles depends on appropriate interactions and function between oocytes and their surrounding granulosa cells. Previously, we showed that double knockout of *Irx3* and *Irx5* (*Irx3/5* DKO) in mice resulted in abnormal follicle morphology and follicle death. Further, female mouse models of individual *Irx3* or *Irx5* knockouts were both subfertile but with distinct defects. Notably, the expression profile of each gene suggests independent roles for each; first, they are colocalized in pre-granulosa cells during development that then progresses to include oocyte expression during germline nest breakdown and primordial follicle formation. Thereafter, their expression patterns diverge between oocytes and granulosa cells coinciding with the formulation and maturation of intimate oocyte–granulosa cell interactions. The objective of this study was to investigate the contributions of *Irx5* and somatic cell-specific expression of *Irx3* during ovarian development. Our results show that *Irx3* and *Irx5* contribute to female fertility through different mechanisms and that *Irx3* expression in somatic cells is important for oocyte quality and survival. Based on evaluation of a series of genetically modified mouse models, we conclude that IRX3 and IRX5 collaborate in the same cells and then in neighboring cells to foster a healthy and responsive follicle. Long after these two factors have extinguished, their legacy enables these intercellular connections to mature and respond to extracellular signals to promote follicle maturation and ovulation.

© The Author(s) 2020. Published by Oxford University Press on behalf of Society for the Study of Reproduction. All rights reserved.
For permissions, please e-mail: journals.permissions@oup.com

Summary Sentence

IRX3 and IRX5 collaborate in the same and then in neighboring cells to foster the extension of cellular processes that connect the oocyte and neighboring granulosa cells within the primordial follicle to promote follicle integrity.

Key words: ovary, primordial follicle, ovary development, Irx3, Irx5, granulosa cell, pre-granulosa cell, oocyte, follicle.

Introduction

Ovarian follicle development relies on productive communication between the oocyte and its neighboring granulosa cells, primarily via direct communication [1–3]. While these networks are not required until a follicle is activated, the foundation for oocyte–granulosa cell communication is laid upon primordial follicle formation. Primordial follicles are formed as a result of germline nest breakdown by week 20 in humans and around the time of birth in rodents [4–6] by a process that is largely unknown, but under intense investigation. Once these follicles have formed, most remain dormant for months and up to several decades in humans. Each retains the remarkable capacity to respond to activation signals at any given time, although few follicles are destined to survive to ovulation. Ultimately, the infrastructure for oocyte–granulosa cell communication is generated by factors that are expressed during early stages of ovary development that disappear, but leave a legacy to ensure a coordinated and timely response to a future call. Previously, we reported that synchronized activity and timing of two members of the Iroquois homeobox transcription factor family, *Irx3* and *Irx5*, correspond to the development of oocyte–granulosa cell interactions during primordial follicle formation suggesting that they play important roles as legacy factors for future intrafollicle communication.

IRX3 and IRX5 are two of the six members of the Iroquois family of proteins in mammals that is defined by an 11-amino acid *Iro* motif and inclusion of a three amino acid loop extension (TALE) within the homeobox DNA binding domain [7, 8]. These two factors have been shown to collaborate to promote development of several organ systems including the heart, gastrointestinal tract, spinal cord, limb, kidney, and mammary gland [9–13]. Loss of both *Irx3* and *Irx5* causes embryonic lethality, but evaluation of postnatal mutant and wild-type ovaries was achieved by kidney capsule transplantation of embryonic ovaries, which showed that both genes are essential for follicle and oocyte survival [14]. Further, fertility of both *Irx3*-($Irx3^{LacZ/LacZ}$, *Irx3* KO) and *Irx5* single knockout ($Irx5^{EGFP/EGFP}$, *Irx5* KO) females was affected but in different ways, suggesting that each factor has a distinct contribution to female fertility [14]. Indeed, we observed that *Irx3* and *Irx5* exhibit spatiotemporal expression profiles that exemplify the interwoven nature of somatic cells and oocytes within the developing mouse ovary. Both genes are co-expressed in somatic cells (pre-granulosa cells) within germline nests during gestation and then also appear in oocytes at the onset of germline nest breakdown and primordial follicle formation [14]. After the primordial follicle stage, *Irx3* and *Irx5* diverge in their expression patterns with *Irx5* reverting back to granulosa cell-only expression briefly before being extinguished, and *Irx3* transitioning to oocyte-specific expression that is maintained. These expression patterns suggest deliberate collaborations that are not yet understood.

Based on these data, we hypothesize that *Irx3* contributes to ovarian development via activity within both pre-granulosa cells and oocytes whereas *Irx5* functions predominantly through its pre-granulosa cell-specific expression. Both perform functions during development that set the stage for future follicle health long after they are no longer present. Our objective for this study was to investigate the somatic or granulosa cell contribution of both factors using an array of genetically modified mouse models. First, we extended *Irx3* expression within the granulosa cell population in advanced stage follicles and observed no impact of fertility. Second, we generated mice to target deletion of *Irx3* from somatic cells in the context of the *Irx5* KO ($Sf1Cre^{+}$; $Irx3^{flox}Irx5^{EGFP}/Irx3^{flox}Irx5^{EGFP}$ or *Irx3* sKO) and found that these females ovulated fewer oocytes than the controls, but they did not increase the deficit in pup accumulation seen in *Irx5* KO females. Finally, we took an additional step with *Irx3* sKO mice by layering the loss of one *Irx3* allele within oocytes ($Sf1Cre^{+}$;$Irx3^{flox}Irx5^{EGFP}/Irx3^{-}Irx5^{EGFP}$ referred to as $Sf1Cre^{+}$ Haplo-mutant). These females exhibited a more profound reduction in oocyte ovulation along with additional follicle growth deficits. Altogether, results from these studies indicate that the legacy impact of *Irx5* on female fertility resides within the timeframe between ovulation and embryo implantation while somatic cell-derived *Irx3* contributes to the follicle response to growth and ovulation signals. In addition, these studies point to a critical function of *Irx3* within the oocyte, which will be the focus of future studies.

Materials and methods

Ethics statement

Adult animals were euthanized by CO_2 asphyxiation followed by cervical dislocation. Embryonic pups were euthanized by decapitation with a razor blade. Animal housing and all procedures described were reviewed and approved by the Institutional Animal Care and Use Committee at the University of Wisconsin–Madison and were performed in accordance with National Institute of Health Guiding Principles for the Care and Use of Laboratory Animals.

Animals

Mouse strains included CD1 outbred mice (Crl:CD1(ICR), Charles River, Wilmington MA), $Irx3^{flox}Irx5^{EGFP}$ [15], $Irx3^{-}Irx5^{EGFP}$ [15], *Sf1Cre* (Tg(Nr5a1-cre)2Klp, Jackson Labs, Bar Harbor, ME), originally obtained from the Keith Parker Lab (deceased), and ROSA26-$Stop^{flox}$/Irx3-IRES-EGFP mice (referenced as $Irx3^{GOF}$), generated and provided by Dr Chi-chung Hui, University of Toronto, with *Irx3* sequences inserted behind the Rosa26 promoter within the Rosa locus with a floxed stop codon. *Sf1Cre* mice were maintained on a C57BL/6 J genetic background, while all other mice were maintained on a CD1 genetic background. Genotyping for *Sf1Cre*, $Irx5^{EGFP}$, and $Irx3^{-}Irx5^{EGFP}$ was carried out as previously reported [15, 16]. CD1 males were used to pair with females for breeding studies and timed pregnancy. Timed mating was identified by the presence of a vaginal plug, which was designated as embryonic day 0.5 (E0.5).

Histology and follicle quantification

Ovaries were harvested at the specified age point indicated, fixed in 4% paraformaldehyde overnight, rinsed and then embedded in paraffin. Blocks were sectioned at 8 µm thickness, selected slides were stained with hematoxylin and eosin (H&E) for histological analysis. Ovaries used for follicle quantification were sectioned through completely, and every 10th section was used to quantify the structures in ovary. The number of follicles at different developmental stages, corporal lutea (CLs), as well as atretic follicles were recorded. CLs and large follicles were counted in each quantified section for every ovary; therefore, these structures were counted multiple times resulting in the high numbers/ovary. Follicles that were atretic at or before secondary follicle stage were considered as small atretic follicles, while those that showed atretic signs at preantral stage and beyond were considered as large atretic follicles. Investigators blinded to the ovary genotypes completed all quantifications.

RNA extraction and real-time quantitative polymerase chain reaction

RNA was extracted using RNeasy Micro Kit (Qiagen, Germantown, MD) according to the manufacturer's instructions and quantified using a NanoDrop 2000. Five hundred nanograms of RNA from each sample were used for First-Strand cDNA (complementary DNA) synthesis by SuperScriptII-RT (Invitrogen, AM9515, Carlsbad, CA). Complementary DNA was diluted 1:5 and then 2 µL was added to 5 µL SYBR green polymerase chain reaction (PCR) mixture (BioRad, cat #1725271, Hercules, CA), 2.4 µL water, and 1.25 pmol primer mix. PCR reactions were carried out using the BioRad CFX96 system. RNA transcripts were quantified using the ΔΔCt method [17]. Briefly, to control for overall gene expression in each time point, the average cycle threshold (aveCt) for 36B4 was subtracted from the aveCt value for each gene to generate ΔCt. Next, ΔCt for each gene was compared to ΔCt of that same gene for the mutant genotype (e.g., $\Delta Ct\ Irx3_{\text{female control}} - \Delta Ct\ Irx3_{\text{female mutant}}$), to generate ΔΔCt. Finally, fold change was calculated as 2 to the $-\Delta\Delta Ct$ power ($2^{-\Delta\Delta Ct}$). Primers are listed in Supplementary data, Table S1.

Fertility studies

Sf1Cre^{+};*Irx3*$^{GOF/GOF}$ and No Cre;*Irx3*$^{GOF/GOF}$ in addition to *Irx3* sKO, No Cre mutant (*Irx5* KO) and littermate control female mice were set up with wild-type (CD1) males for 6 months. Each female was exposed to two to three different males. Litter sizes and birth dates were recorded throughout the breeding period.

Because of their small size and ill thrift, reproductive fitness for *Sf1Cre*$^{+}$ Haplo-mutant (previously referred to as Hypomorph, [14]) and No Cre Haplo-mutant mice was evaluated at 8-weeks of age using a superovulation protocol followed by in vitro fertilization (IVF) and analysis of fertilization up to the two-cell stage. This requires that the mouse reaches at least 10 g of weight before starting the hormone induction. The superovulation protocol included an intraperitoneal injection of 5 IU of pregnant mare's serum gonadotropin followed by 5 IU of human chorionic gonadotropin (hCG) 48 h later. Sixteen hours after the hCG injection, oocytes were extracted from the oviduct and uterus and in vitro fertilized with sperm from CD1 males. The fertilized oocytes were cultured to reach the two-cell embryo stage. The number of ovulated oocytes, fragmented oocytes, oocytes used for IVF, and two-cell embryos postfertilization were recorded. The two-cell efficiency was calculated by dividing the two-cell embryo number by the number of oocytes subjected to IVF for each animal. Due to the variability across superovulation and IVF experiments, each number presented was normalized relative to control data within each experiment.

Statistical analyses

Statistical evaluation of superovulation, IVF, breeding study, follicle quantification, and RT-qPCR results between groups were carried out using a one-way ANOVA and one-tailed *t*-test assuming unequal variances. Results were considered statistically different if *P*-values were ≤ 0.05. Results of $P < 0.1$ are also reported as a trend.

Results

Irx5 null female mice are subfertile without significant ovarian defects

Previously, we determined that follicles in *Irx3*$^{-}$*Irx5*^{EGFP}/*Irx3*$^{-}$*Irx5*^{EGFP} (*Irx3/5* DKO) ovaries die due to disrupted granulosa cell–oocyte interactions [14, 18]. In addition, targeted disruption of each individual factor (*Irx3*$^{LacZ/LacZ}$, *Irx3* KO; *Irx5*$^{EGFP/EGFP}$, *Irx5* KO) resulted in subfertility, but with different patterns suggesting distinct roles for each [14]. Indeed, cell localization of *Irx3* and *Irx5* shows distinct and dynamic patterns during ovary development. Both factors colocalize to pre-granulosa cells of germline nests and then expand to oocytes upon germline nest breakdown. Thereafter, *Irx3* expression becomes confined to oocytes where it remains while *Irx5* expression reverts to pre-granulosa and then granulosa cells before it is extinguished by the time of puberty [14]. Our previous report showed that there was no difference in histology or follicle structure quantification between *Irx5* KO and control ovaries of 8-month-old mice following a 6-month breeding trial [14]. To understand the impact of *Irx5* KO on female fertility, we expanded our evaluation of follicle populations and examined other aspects of the reproductive axis of *Irx5* KO mice and their littermate controls over time.

Histological analysis of *Irx5* KO ovaries showed that like the 8-month ovaries, morphology and ovarian composition of 3-week (Figure 1A'), 3-month (Figure 1B'), and 6-month (Figure 1C') mutant ovaries were comparable to those of their littermate controls (Figure 1A–C). In addition, quantification of ovarian structures over time was not significantly different between *Irx5* KO mutant and the control mice. We observed a similar developmental trend that included a decreasing primordial follicle pool that corresponded to an increase in corpora lutea (CL) and atretic follicle counts as they aged (Figure 1A"–C"). To explain these outcomes, we investigated whether *Irx3* expression was compensating for the lack of *Irx5* in *Irx5* KO ovaries. Results from quantitative reverse transcriptase PCR (qRT-PCR) in developing ovaries showed that while *Irx5* transcripts were undetectable as expected, *Irx3* expression was no different in *Irx5* KO compared to wild-type control (Supplementary data, Figure S1).

Besides the ovary, other organs of the reproductive axis are critical to female fertility and include the uterus, hypothalamus, and pituitary. Each of these tissues was harvested from adult control females and processed for qRT-PCR. Results show that *Irx5* transcripts were not detected in the pituitary or uterus (Supplementary data, Figure S2A and B). In addition, immunofluorescence for the EGFP reporter was not detected in adult uteri of *Irx5*$^{EGFP/+}$ mice (Supplementary data, Figure S2C and D'). In contrast, *Irx5* expression in the hypothalamus was comparable to that of the developing ovary (positive control; Supplementary data, Figure S2B). Previous reports have identified *Irx5* as a marker of the supramammilary

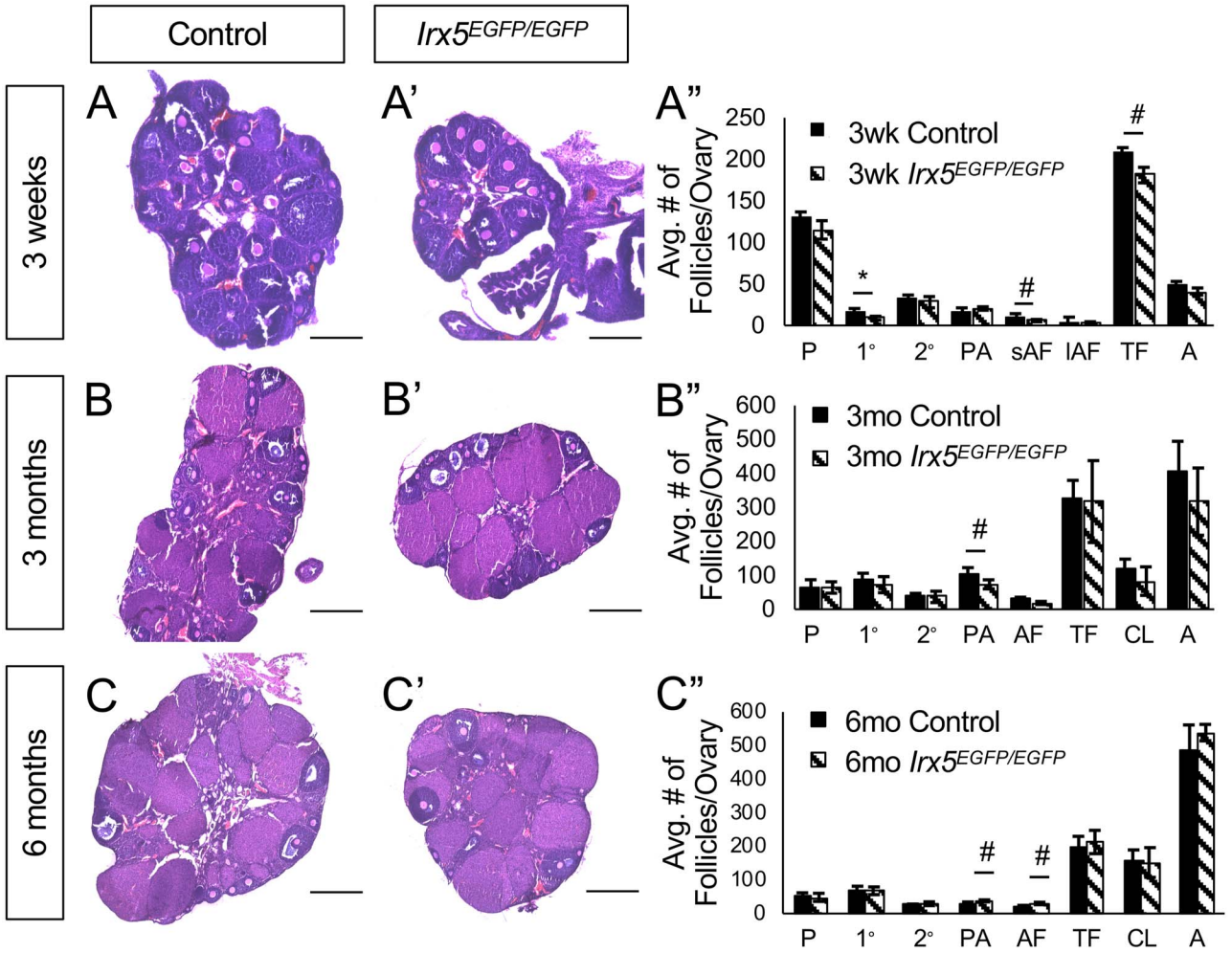

Figure 1. Histology and follicle structures between control and *Irx5* KO ovaries are similar. (A–C′) H&E staining of 3-week ($n = 3$ for each group), 3-month ($n = 3$ for each group), and 6-month ($n = 3$ for each group) old control (A–C) and *Irx5* KO ($Irx5^{EGFP/EGFP}$) (A′–C′) ovaries. Ovaries of 3-month and 6-month mice were harvested at 6.5 days of gestation (E6.5). Scale bars represent 250 μm. (A″–C″) Follicles of different development stages were quantified at each age point. P: primordial follicle; 1°: primary follicle; 2°: secondary follicle; PA: preantral follicle; sAF: small antral follicle; lAF: large antral follicle, AF: antral follicle; TF: total follicle, A: atretic follicle. Data in A″–C″ represent the mean ± SEM. Statistics: two-sample *t*-test; $^{*}P < 0.05$; $^{**}P < 0.01$; $^{\#}P < 0.1$.

nucleus of the hypothalamus [19–21]; however, there is no indication that *Irx5* is present in gonadotropin-releasing hormone neurons. Altogether, these data show that a global deficit of *Irx5* causes subfertility; however, evaluation of its function and expression profile in reproductive axis organs failed to explain this phenotype. Given that *Irx5* is predominantly expressed within somatic (pre-granulosa) cells, we therefore turned to investigate somatic cell-specific contributions of *Irx3* alone, and in the context of the *Irx5* KO to increase our understanding of their combined action within these cells.

Extending *Irx3* expression within somatic cells does not affect female or male fertility

Following germline nest breakdown and primordial follicle formation, *Irx5* expression resumes granulosa cell-specific expression while *Irx3* becomes confined to the oocyte [14]. To investigate the consequences of prolonging *Irx3* expression within somatic cells of the ovary starting during development, we bred *Sf1Cre* [22] to *Rosa26-Irx3-EGFP* gain of function ($Irx3^{GOF/GOF}$) mice. $Sf1Cre^{+}$;$Irx3^{GOF/GOF}$ and No Cre;$Irx3^{GOF/GOF}$ (No Cre control) ovaries were harvested from embryonic day (E) 15.5, E16.5, postnatal day (P) 0, P21, and adult mice to follow ovarian development and follicle maturation over time. Gain of *Irx3* expression was validated by measuring transcripts from E15.5 ovaries, when *Irx3* and *Irx5* are confined to pre-granulosa cells. *Irx3* transcripts increased by 2-fold while no changes were detected in expression of *Rps29* (negative control), *Foxl2* (female somatic cell marker), or *Irx5* (Figure 2A). Morphological analysis of ovaries over time showed the presence of healthy follicles of all stages in both $Sf1Cre^{+}$;$Irx3^{GOF/GOF}$ and No Cre control ovaries (Figure 2B). Finally, $Sf1Cre^{+}$;$Irx3^{GOF/GOF}$ and No Cre control females were paired with wild-type CD1 males over 6 months to assess fertility. Litter birthdates and pup numbers were recorded throughout the breeding period and showed no significant differences between groups (Figure 2C).

Irx3 is not expressed at any point during testis development; therefore, we hypothesized that aberrant *Irx3* overexpression may cause defects in testis development and/or male fertility. Testes were collected at E15.5, E16.5, P0, P21, and adult stages to analyze testis

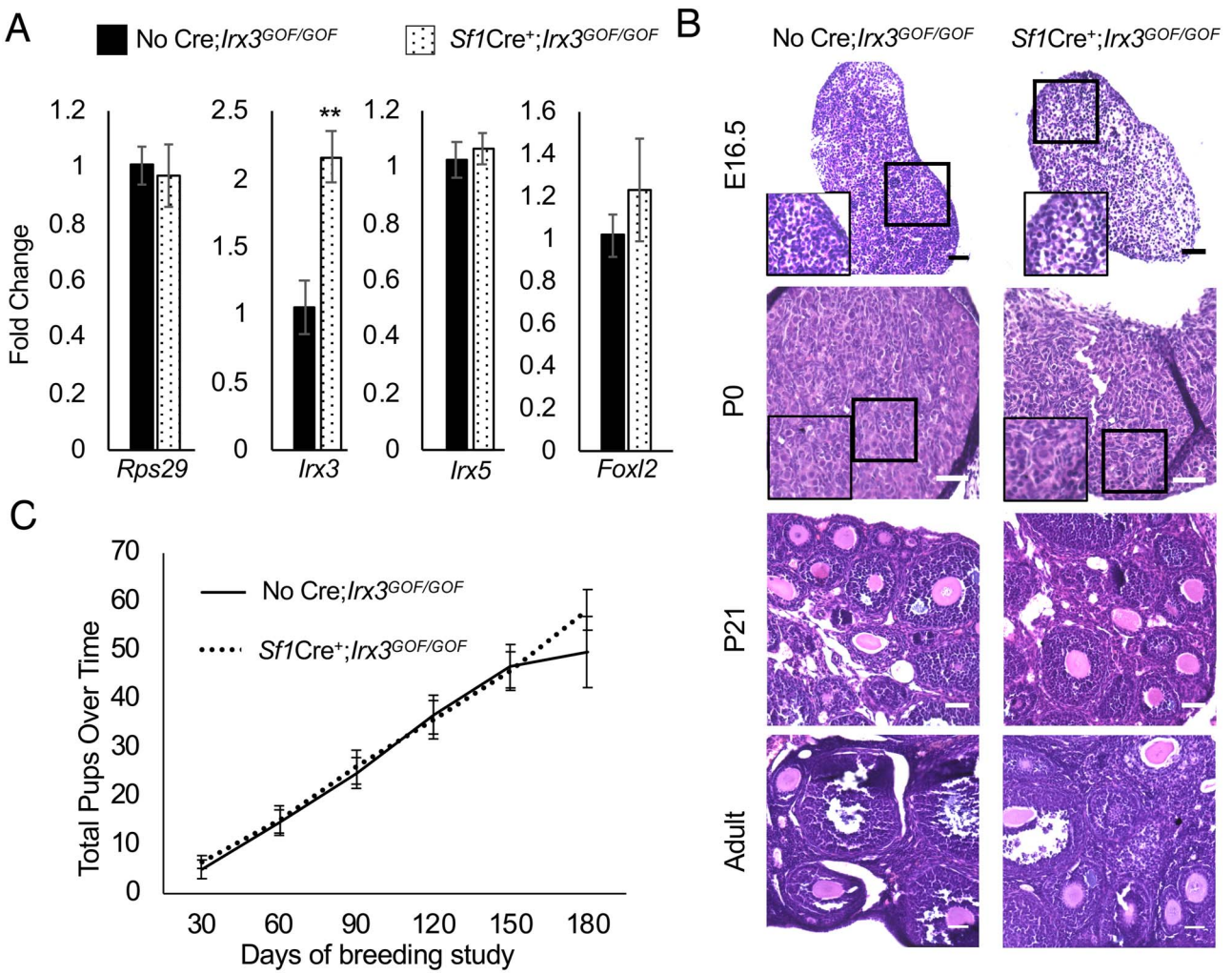

Figure 2. *Irx3* overexpression in somatic cells of the ovary does not affect follicle formation, maturation or fertility. (A) qPCR validation of *Irx3* overexpression. *Rps29* represents a negative control. Results are reported relative to No Cre;$Irx3^{GOF/GOF}$ for each gene. (B) H&E images of ovaries at indicated time points in control (No Cre;$Irx3^{GOF/GOF}$) and mutant ($Sf1Cre^{+}$;$Irx3^{GOF/GOF}$) animals. Insets represent higher magnification images of the black boxes. Scale bars represent 50 µm. (C) Control ($n = 5$) and mutant ($n = 4$) females were bred to wild-type male mice for 6 months and the number of pups in each litter were added as they accumulated over time. Data are represented as average ± SEM. $^{**}P < 0.01$.

cord formation and development in $Sf1Cre^{+}$;$Irx3^{GOF/GOF}$ and No Cre control male mice. *Sf1Cre* successfully targeted expression of *Irx3* without impacting *Rps29* (negative control), *Sox9* (somatic cell male marker), or *Irx5* in E15.5 testes (Supplementary data, Figure S3A). Similar to results in female mice, histological analysis showed testis cords and seminiferous tubules in $Sf1Cre^{+}$;$Irx3^{GOF/GOF}$ males that were comparable to controls throughout development and into adulthood (Supplementary data, Figure S3B). Further, a 6-month breeding study was initiated by mating $Sf1Cre^{+}$;$Irx3^{GOF/GOF}$ and No Cre control males with wild-type CD1 females. Results showed no difference in litter sizes over time between the two groups (Supplementary data, Figure S3C). Altogether, these data indicate that *Irx3* overexpression in the somatic cells of the ovary or testis has no impact on organ development or fertility.

Loss of *Irx3* in pre-granulosa cells affects ovulation but does not further impair fertility of *Irx5* KO female mice

Next, to delineate the contribution of somatic cell expression of *Irx3* in ovary development and female fertility within the context of the *Irx5* global knockout, we bred *Sf1Cre* to $Irx3^{flox}Irx5^{EGFP}$/$Irx3^{flox}Irx5^{EGFP}$ mice to generate $Sf1Cre^{+}$; $Irx3^{flox}Irx5^{EGFP}$/$Irx3^{flox}Irx5^{EGFP}$ (herein referred to as *Irx3* somatic cell KO, *Irx3* sKO), No Cre;$Irx3^{flox}Irx5^{EGFP}$/$Irx3^{flox}Irx5^{EGFP}$ (No Cre mutant, also known as *Irx5* KO) and controls. Controls included: (1) $Sf1Cre^{+}$;$Irx3^{+}Irx5^{+}$/$Irx3^{+}Irx5^{+}$ ($Sf1Cre^{+}$ wild type), (2) No Cre;$Irx3^{flox}Irx5^{EGFP}$/$Irx3^{+}Irx5^{+}$ (No Cre het), and (3) $Irx3^{+}Irx5^{+}$/$Irx3^{+}Irx5^{+}$ (wild type) littermates (see schematic in Supplementary data, Figure S4). Control animals were not different from each other and were therefore grouped together. RNA was harvested from E15.5 ovaries and qRT-PCR results validated loss of *Irx3* (and *Irx5*) in $Sf1Cre^{+}$ mutants (Supplementary data, Figure S5). As we have shown in Supplementary data, Figure S1, *Irx3* expression was not affected in $Irx5^{EGFP/EGFP}$ (without *Sf1Cre*) ovaries further demonstrating the specificity and efficiency of *Sf1Cre* targeting floxed *Irx3* alleles in ovary.

As the supporting cells for oocytes, ovarian somatic cells are essential for various aspects of follicle and oocyte development, including cell–cell communication and responses to external signals.

We have previously shown that *Irx3* is expressed in the pre-granulosa cell population only during germline nest and follicle formation stages [14]. It is still premature to conclude whether the prominent somatic cell expression of *Irx3* during this period will have a lasting impact on granulosa cell functions; therefore, we examined the adult stage ovaries for morphology and follicle stage quantification. Histological analysis revealed that *Irx3* sKO ovaries contained fewer CL than their littermate controls (Figure 3A). In addition, follicle quantification confirmed that CL numbers from *Irx3* sKO ovaries were substantially lower than the control and No Cre mutant (*Irx5* KO) ovaries (Figure 3B).

To assess fertility, 6-week-old females were placed in a breeding study for 6 months. Results showed that *Irx3* sKO females (dotted line) produced significantly fewer pups over time compared to their controls (solid line, Figure 3C). When compared to the No Cre mutants (*Irx5* KO), however, *Irx3* sKO fertility was not different, suggesting that somatic cell loss of *Irx3* did not exacerbate the already compromised fertility of *Irx5* KO female mice.

Sf1Cre^{+}*; Irx3/5* Haplo-mutant mice uncover a potential role for oocyte expression of *Irx3*

Irx3 sKO ovaries harbored fewer CL counts suggesting altered granulosa cell–oocyte communication; however, female fertility is no different from *Irx5* KO, suggesting additional roles for *Irx3*. Previously, we reported that mice with only one allele of *Irx3* remaining in the *Irx3* and *Irx5* cluster ($Irx3^{flox}Irx5^{EGFP}/Irx3^{-}Irx5^{EGFP}$, referred to as *Irx3/5* Haplo-mutant) had significant ovulation defects based on quantification of rare CLs [14]. We proceeded to breed *Sf1Cre* into these mice to target deletion of the remaining allele of *Irx3* in granulosa cells ($Sf1Cre^{+}$;$Irx3^{flox}Irx5^{EGFP}/Irx3^{-}Irx5^{EGFP}$ referred to as $Sf1Cre^{+}$ Haplo-mutant), No Cre;$Irx3^{flox}Irx5^{EGFP}/Irx3^{-}Irx5^{EGFP}$ (No Cre Haplo-mutant), and controls. Controls included: (1) $Sf1Cre^{+}$;$Irx3^{+}Irx5^{+}/Irx3^{+}Irx5^{+}$ ($Sf1Cre^{+}$ wild type), (2) No Cre;$Irx3^{flox}Irx5^{EGFP}/Irx3^{+}Irx5^{+}$, (3) No Cre;$Irx3^{+}Irx5^{+}/Irx3^{-}Irx5^{EGFP}$ (2 and 3, No Cre hets), and (4) $Irx3^{+}Irx5^{+}/Irx3^{+}Irx5^{+}$ (wild type) genotypes (see schematic of genotypes, Supplementary data, Figure S4). Control animals were not significantly different from each other and were therefore combined together and referred to as controls.

In general, both $Sf1Cre^{+}$ and No Cre Haplo-mutants were small and frail; therefore, we evaluated fertility using IVF-derived oocyte analysis followed by ovarian histology and structure quantification by 8 weeks of age. Based on histology, $Sf1Cre^{+}$ Haplo-mutant mice had ovaries that were visibly smaller than those of the No Cre Haplo-mutant and control mice. Their small size was attributed to the observation that CL were rarely observed (Figure 4A). Quantification of ovarian structures revealed that $Sf1Cre^{+}$ Haplo-mutant ovaries had a significantly reduced number of CL compared to the littermate controls but the counts were no different than the No Cre Haplo-mutants (Figure 4B). In addition, $Sf1Cre^{+}$ Haplo-mutant ovaries had a significantly higher number of primordial follicles, lower number of secondary and preantral follicles, and a lower number of atretic follicles compared to the littermate controls (Figure 4B). In comparison with the No Cre Haplo-mutant ovaries, there was also a trend of decreased number of secondary and preantral follicles in $Sf1Cre^{+}$ Haplo-mutant ovaries (Figure 4B).

The superovulation protocol produced significantly fewer oocytes from $Sf1Cre^{+}$ Haplo-mutant female mice compared to both No Cre Haplo-mutant and littermate controls (Figure 4C). Healthy oocytes were subject to IVF and the yield of two-cell embryos were comparable between $Sf1Cre^{+}$ and No Cre Haplo-mutants, but these groups were both significantly lower than that of the littermate control group. Ultimately, the efficiency of progression from fertilized egg to two-cell embryo was similar among all three groups (Figure 4C). Together, these data indicate that the inclusion of an *Irx3* deficit in the oocyte within the context of *Irx3* and *Irx5* double KO in granulosa cells exacerbates an insufficient integrated hormone response between granulosa cells and the oocyte to external ovulation signals.

Discussion

IRX3 and IRX5 collaborate within the same and neighboring cells to promote development of many organs, including the spinal cord, heart, and kidney, to name a few [10, 12, 15]. It has emerged that Iroquois factors may work individually or together in cell and tissue specific contexts; therefore, teasing out their specific roles within defined locations has proved challenging [9, 13, 15, 23–25]. Previously, we demonstrated that loss of both *Irx3* and *Irx5* caused abnormal granulosa cell–oocyte contacts within follicles resulting in follicle and oocyte death [14, 18]. Loss of *Irx3* alone caused reduced follicle numbers and lasting impairment of fertility, while the single knockout of *Irx5* resulted in subfertility later in life without a significant ovarian phenotype. Results from this current study reinforced the intricate relationship between the two factors, especially within granulosa cells of the follicle unit.

Irx5-specific contributions to female fertility

Previously, we demonstrated a prominent expression profile of *Irx5* in the ovary and showed that *Irx5* KO females are subfertile [14]. To our surprise, histology of *Irx5* KO ovaries from puberty to adulthood followed a similar developmental pattern with the control ovaries. In addition, we did not detect an obvious role for *Irx5* in reproductive axis tissues from adult females. Questions remain regarding *Irx5* KO subfertility and alternative explanations may include impaired oocyte quality and related early embryo survival defects. Oocyte quality is critical for embryo survival, especially during the early stages of embryo development [26]. Further, histological analysis of follicles may not necessarily reflect the quality or competence of the oocyte. It is known that the microenvironment of the developing oocyte determines its developmental potential [27]. The expression profile for *Irx5* suggests that it—along with *Irx3*—facilitate granulosa cell coordination with the oocyte [14]. Additional evaluation of ovulated oocytes and early embryo survival in *Irx5* KO mice will help us further determine the contributions of *Irx5* to female fertility.

Manipulation of somatic cell-specific *Irx3* expression illuminates distinct and collaborative roles with *Irx5*

Irx3 and *Irx5* are absent in the developing testis but co-localize in somatic cells that mark the pre-granulosa cell population in the developing ovary until primordial follicles have formed. *Irx5* expression persists in granulosa cells without *Irx3* for a brief time after birth. During this time, *Irx3* transitions to oocyte-only expression [14]. We challenged this profile by generating mice with somatic cell-targeted ectopic production of *Irx3* that facilitated expression within the testis and maintained expression in postnatal granulosa cells in the ovary. To our surprise, we observed normal morphology and fertility in mutant mice of both sexes. It is possible that ectopic expression of *Irx3* is not important. Alternatively, in both testis and ovary, we posit that the full impact of *Irx3* expression cannot be

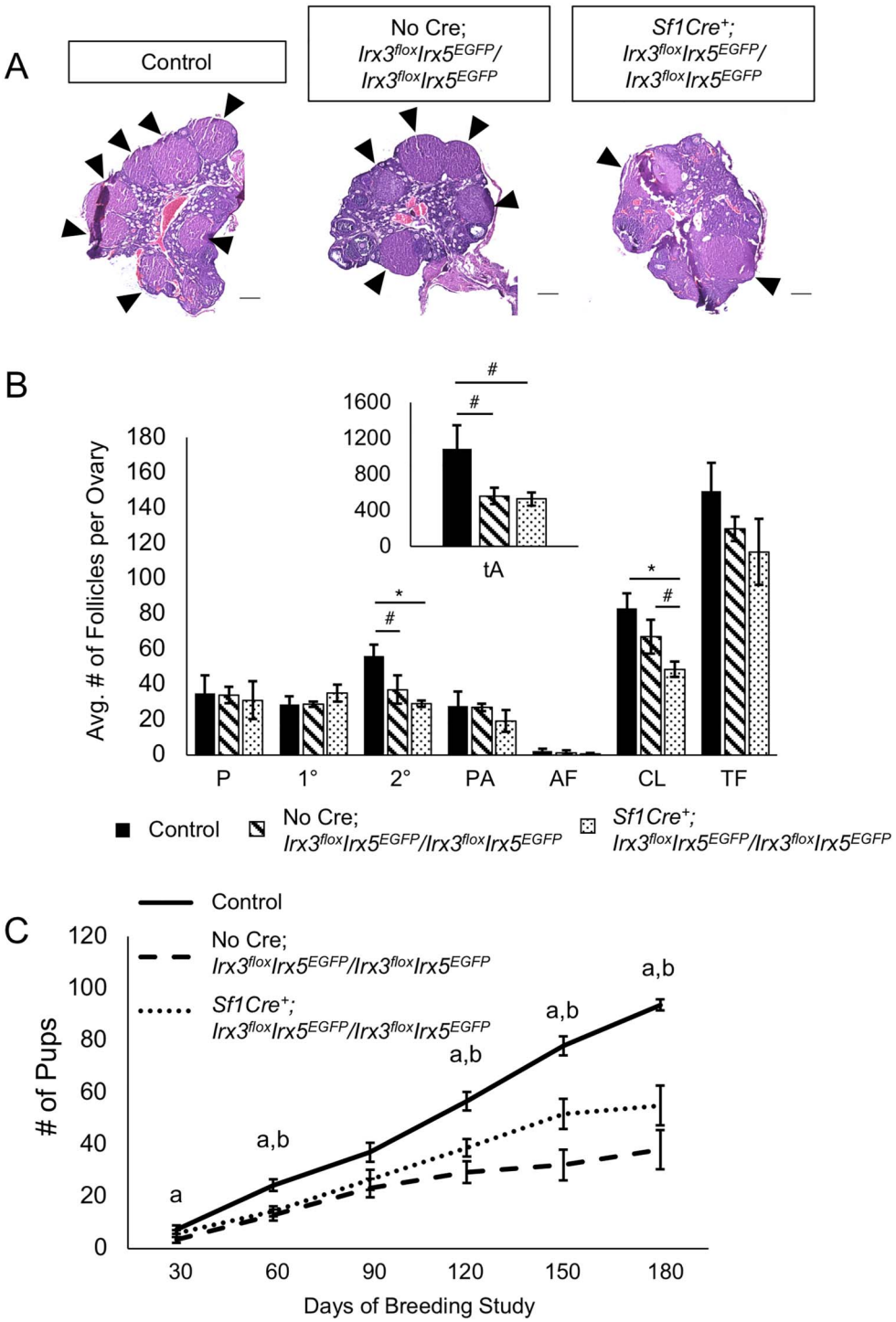

Figure 3. Somatic cell specific knockout of *Irx3* causes subfertility and ovarian defects in female mice. (A) H&E histology of control, *Irx5* KO (No Cre;*Irx3*^{flox}*Irx5*^{EGFP}/*Irx3*^{flox}*Irx5*^{EGFP}) and *Irx3* sKO (*Sf1Cre*$^{+}$;*Irx3*^{flox}*Irx5*^{EGFP}/*Irx3*^{flox}*Irx5*^{EGFP}) ovaries. Scale bars represent 250 μm. (B) Quantification of ovarian structures in ovaries of control, *Irx5* KO, and *Irx3* sKO ($n = 3$ for each group). P: primordial follicle; 1°: primary follicle; 2°: secondary follicle; PA: preantral follicle; AF: antral follicle; CL: corpus luteum; TF: total follicles excluding atretic follicles; tA: total atretic follicles. (C) Breeding study results are reported as the accumulated number of pups from *Irx5* KO ($n = 13$) and *Irx3* sKO ($n = 11$) females versus littermate control females ($n = 13$) during a 6-month (180 days) period. Data in B and C represent the mean ± SEM. Statistics: one-way ANOVA and two-sample *t*-test; a: Difference between the control and No Cre group is significant ($P < 0.05$); b: Differences between the control and *Sf1Cre*$^{+}$ groups are significant ($P < 0.05$).

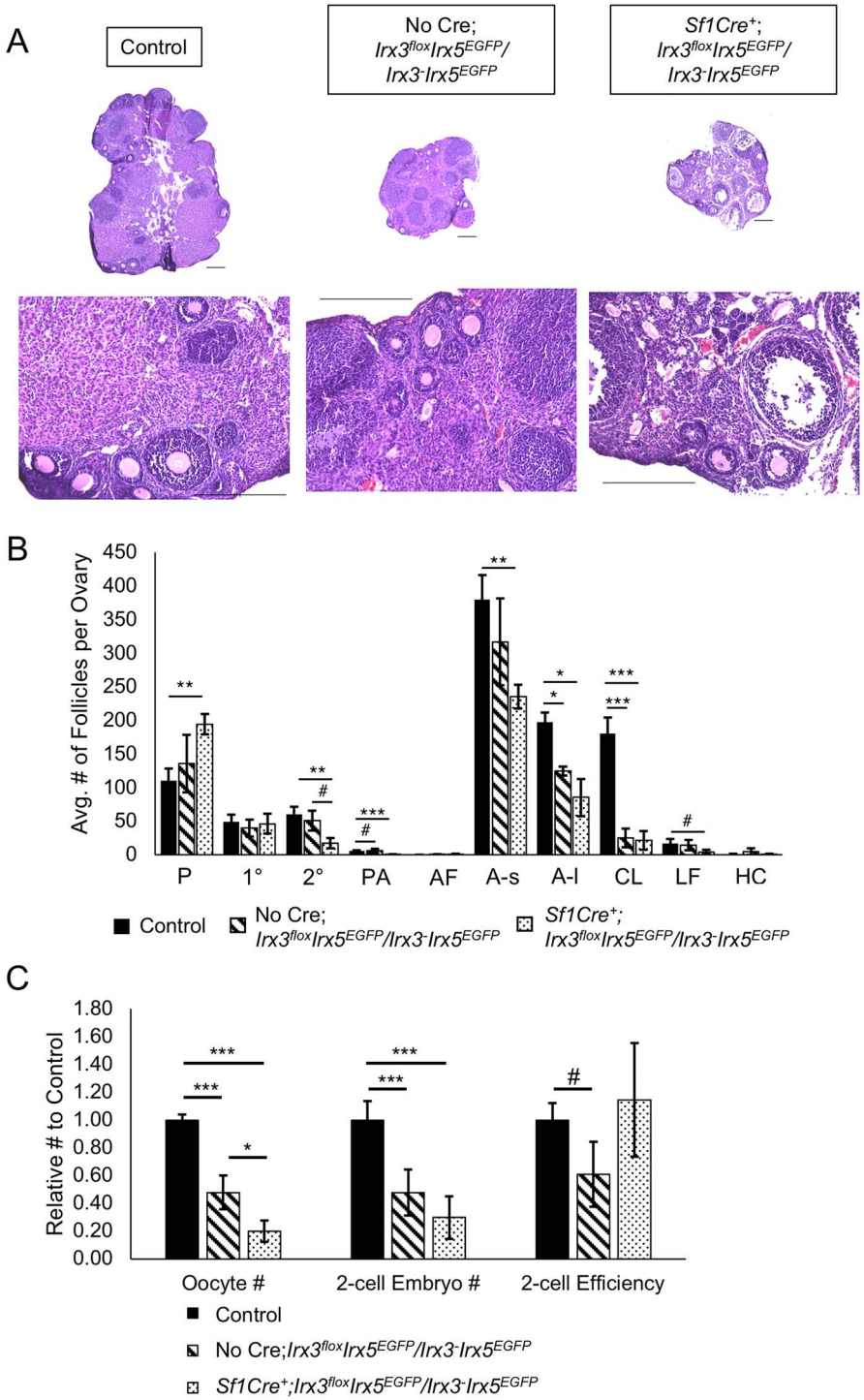

Figure 4. Somatic cell specific *Irx3* knockout in *Sf1Cre*$^{+}$ Haplo-mutant mice results in subfertility and ovarian follicle development defects. (A) H&E histology of control ($n = 6$), No Cre;*Irx3*^{flox}*Irx5*^{EGFP}/*Irx3*$^{-}$ *Irx5*^{EGFP} (No Cre Haplo-mutant; $n = 3$) and *Sf1Cre*$^{+}$;*Irx3*^{flox}*Irx5*^{EGFP}/*Irx3*$^{-}$ *Irx5*^{EGFP} (*Sf1Cre*$^{+}$ Haplo-mutant; $n = 3$) ovaries. Under each ovary, the H&E images show follicles at different developmental stages at a higher magnification. Scale bars represent 250 μm. (B) Quantification of ovarian structures in control, No Cre Haplo-mutant, and *SF1Cre*$^{+}$ Haplo-mutantovaries ($n = 3$ each). P: primordial follicle; 1°: primary follicle; 2°: secondary follicle; PA: preantral follicle; AF: antral follicle; A-s: small atretic follicle (primordial to secondary stage); A-l: large atretic follicle (preantral stage and beyond); CL: corpus luteum; LF: luteinized follicle; HC: hemorrhagic cyst. (C) Fertility assessment of control, No Cre Haplo-mutant and *Sf1Cre*$^{+}$ Haplo-mutant mice using superovulation and IVF. Graphs represent the number of oocytes retrieved after superovulation, the number of 2-cell embryos counted and the efficiency to develop into two-cell embryos postfertilization. Data in B and C represent the mean ± SEM. Statistics: one-way ANOVA and two-sample *t*-test; $^{*}P < 0.05$; $^{**}P < 0.01$; $^{***}P < 0.001$; $^{\#}P < 0.1$.

appreciated without equal presence of its cognate partner, *Irx5*, and perhaps other cofactors. The basis for this statement is supported by other studies that demonstrated collaboration between *Irx3* and *Irx5* during development and the evidence for IRX factors' transcriptional control requiring their binding to DNA as heterodimers [7, 10, 12, 15, 28]. Our stepwise approach to eliminate somatic cell expression of *Irx3* in the context of a global *Irx5* KO was used to evaluate this further within the developing ovary.

Both *Irx3* sKO and *Sf1Cre*$^{+}$ Haplo-mutant ovaries exhibited decreased numbers of growing follicles and CL suggesting that defective granulosa cell–oocyte interactions contributed to the reduced fertility in these mice. Coordination of follicle maturation and ovulation depend upon upregulation of receptors for follicle stimulating hormone (FSH) and luteinizing hormone (LH) [14, 29, 30]. Previous studies have shown that the granulosa cell response to ovulatory LH signaling involves LH receptors, the mitogen-activated protein kinase (MAPK) pathway, and gap junctions including connexin 37 (GJA4) and connexin 43 (GJA1) to propagate signals [31–39]. Before reaching the preovulatory stage, the MAPK pathway has also been shown to work with cAMP in granulosa cells to respond to FSH signals during follicle maturation [34, 38, 40–42]. Previously, we showed that the *Irx3* and *Irx5* DKO mutation results in abnormal localization of GJA1 in follicles in addition to deficient cellular extensions including transzonal processes from granulosa cells and microvilli from oocytes [14]. Based on these combined data, we propose that somatic cell expression of *Irx3* and *Irx5* during developmental stages leaves a legacy on female fertility by promoting functional intrafollicle cell interactions that set the stage for progressive MAPK signals that coordinate with FSH and LH signals to ensure follicle maturation followed by ovulation.

We are limited in our ability to tease out *Irx3* versus *Irx5* contributions because of the intricate relationship between the two with respect to chromosomal location, regulation, and their emerging collaborative relationship within and between cells. Studies in other systems suggest that IRX3 and IRX5 play compensatory roles in the same and adjacent cells [13, 43]. We did not observe compensation at the transcript level between *Irx5* and *Irx3*; however, further studies at the level of protein activity must be undertaken to further understand their functional interactions. Additional tools—including the ability to evaluate cell-specific activity of each factor individually and together—would be ideal to progress in these studies. Given their proximity within the *IrxB* locus, generation of double knockout or other combinations of mutations between the two genes is complicated. One group of scientists tried to make *Irx3* and *Irx5* double knockout mice using the CRISPR/Cas9 technique with limited success [44]. Ultimately, as more sophisticated techniques become available, our goal will be to evaluate distinct domains of each or both genes such as the *Iro* or TALE domains to understand specific roles for each of them and learn pathways that distinguish this family from other homeodomain factors.

In conclusion, our studies suggest that like other tissues, IRX3 and IRX5 collaborate within the same cell and then in the context of neighboring cells to lay the foundation for the future health and function in the ovary. Both factors leave a legacy of their functions in granulosa cells and likely, also in the oocyte, which is currently under investigation. We have shown that *Irx3* and *Irx5* work together to promote granulosa cell and oocyte cellular extensions and intimate communication to facilitate optimal follicle responses to external signals. These studies have added a new dimension to intrafollicle communication that begins with primordial follicle formation and culminates with ovulation.

Supplementary data

Supplementary data are available at *BIOLRE* online.

Acknowledgements

We thank all members of the Jorgensen laboratory for comments and support. Special thanks are extended to Amanda Vanderplow who contributed to this study during her rotation in our lab. We are grateful for the comments, advice, and technical support from the Developmental Endocrinology Group at the University of Wisconsin–Madison, School of Veterinary Medicine. We would also like to show our gratitude to Jessica Noel, Annie Novak, Jodie Schilling, and Tori Gronemeyer for their exemplary mouse husbandry help.

Author Contributions

A.F., M.L.K., and J.S.J. designed the experiments; A.F., M.L.K., and R.M.B. performed the experiments; A.F., S.A.S., and J.S.J. quantified the follicles; L.W. acquired and processed data and proofread the manuscript; A.F. and K.J.K. performed the superovulation and IVF; X.Z. and C.C.H. generated the transgenic mice used in this study and provided valuable insights for the discussion; A.F., M.L.K., and J.S.J. drafted the manuscript.

References

1. Ackert CL, Gittens JE, O'Brien MJ, Eppig JJ, Kidder GM. Intercellular communication via connexin43 gap junctions is required for ovarian folliculogenesis in the mouse. *Developmental biology* 2001; **233**:258–270.
2. Kidder GM, Vanderhyden BC. Bidirectional communication between oocytes and follicle cells: Ensuring oocyte developmental competence. *Can J Physiol Pharmacol* 2010; **88**:399–413.
3. Matzuk MM, Burns KH, Viveiros MM, Eppig JJ. Intercellular communication in the mammalian ovary: Oocytes carry the conversation. *Science* 2002; **296**:2178–2180.
4. Pepling ME, Spradling AC. Mouse ovarian germ cell cysts undergo programmed breakdown to form primordial follicles. *Dev Biol* 2001; **234**:339–351.
5. Reynaud K, Cortvrindt R, Verlinde F, De Schepper J, Bourgain C, Smitz J. Number of ovarian follicles in human fetuses with the 45,X karyotype. *Fertil Steril* 2004; **81**:1112–1119.
6. Pangas SA, Rajkovic A, Vinci D, Carpi B. *Follicular Development: Mouse, Sheep, and Human Models*. Knobil and Neill's. *Physiology of Reproduction* 2015; 947–995.
7. Bosse A, Stoykova A, Nieselt-Struwe K, Chowdhury K, Copeland NG, Jenkins NA, Gruss P. Identification of a novel mouse Iroquois homeobox gene, Irx5, and chromosomal localisation of all members of the mouse Iroquois gene family. *Dev Dyn* 2000; **218**:160–174.
8. Burglin TR. Analysis of TALE superclass homeobox genes (MEIS, PBC, KNOX, Iroquois, TGIF) reveals a novel domain conserved between plants and animals. *Nucleic Acids Res* 1997; **25**:4173–4180.
9. Gomez-Skarmeta JL, Modolell J. Iroquois genes: Genomic organization and function in vertebrate neural development. *Curr Opin Genet Dev* 2002; **12**:403–408.
10. Cavodeassi F, Modolell J, Gomez-Skarmeta JL. The Iroquois family of genes: From body building to neural patterning. *Development* 2001; **128**:2847–2855.
11. Peters T, Dildrop R, Ausmeier K, Ruther U. Organization of mouse Iroquois homeobox genes in two clusters suggests a conserved regulation and function in vertebrate development. *Genome Res* 2000; **10**:1453–1462.
12. Houweling AC, Dildrop R, Peters T, Mummenhoff J, Moorman AF, Ruther U, Christoffels VM. Gene and cluster-specific expression of the

Iroquois family members during mouse development. *Mech Dev* 2001; **107**:169–174.
13. Holmquist Mengelbier L, Lindell-Munther S, Yasui H, Jansson C, Esfandyari J, Karlsson J, Lau K, Hui CC, Bexell D, Hopyan S, Gisselsson D. The Iroquois homeobox proteins IRX3 and IRX5 have distinct roles in Wilms tumour development and human nephrogenesis. *J Pathol* 2019; **247**:86–98.
14. Fu A, Oberholtzer SM, Bagheri-Fam S, Rastetter RH, Holdreith C, Caceres VL, John SV, Shaw SA, Krentz KJ, Zhang X, Hui CC, Wilhelm D et al. Dynamic expression patterns of Irx3 and Irx5 during germline nest breakdown and primordial follicle formation promote follicle survival in mouse ovaries. *PLoS Genet* 2018; **14**:e1007488.
15. Gaborit N, Sakuma R, Wylie JN, Kim KH, Zhang SS, Hui CC, Bruneau BG. Cooperative and antagonistic roles for Irx3 and Irx5 in cardiac morphogenesis and postnatal physiology. *Development* 2012; **139**:4007–4019.
16. Zhang SS, Kim KH, Rosen A, Smyth JW, Sakuma R, Delgado-Olguin P, Davis M, Chi NC, Puviindran V, Gaborit N, Sukonnik T, Wylie JN et al. Iroquois homeobox gene 3 establishes fast conduction in the cardiac his-Purkinje network. *Proc Natl Acad Sci U S A* 2011; **108**: 13576–13581.
17. Livak KJ, Schmittgen TD. Analysis of relative gene expression data using real-time quantitative PCR and the 2(−Delta Delta C(T)) method. *Methods* 2001; **25**:402–408.
18. Jorgensen JS. Defining the neighborhoods that escort the oocyte through its early life events and into a functional follicle. *Mol Reprod Dev* 2013; **80**:960–976.
19. Shimogori T, Lee DA, Miranda-Angulo A, Yang Y, Wang H, Jiang L, Yoshida AC, Kataoka A, Mashiko H, Avetisyan M, Qi L, Qian J et al. A genomic atlas of mouse hypothalamic development. *Nat Neurosci* 2010; **13**:767–775.
20. Miquelajauregui A, Sandoval-Schaefer T, Martinez-Armenta M, Perez-Martinez L, Carabez A, Zhao Y, Heide M, Alvarez-Bolado G, Varela-Echavarria A. LIM homeobox protein 5 (Lhx5) is essential for mamillary body development. *Front Neuroanat* 2015; **9**:136.
21. Gao Y, Sun T. Molecular regulation of hypothalamic development and physiological functions. *Mol Neurobiol* 2016; **53**:4275–4285.
22. Bingham NC, Verma-Kurvari S, Parada LF, Parker KL. Development of a steroidogenic factor 1/Cre transgenic mouse line. *Genesis (New York, N.Y.: 2000)* 2006; **44**:419–424.
23. Bosse A, Zülch A, Becker M-B, Torres M, Gómez-Skarmeta JL, Modolell J, Gruss P. Identification of the vertebrate Iroquois homeobox gene family with overlapping expression during early development of the nervous system. *Mechanisms of development* 1997; **69**:169–181.
24. Marra AN, Wingert RA. Roles of Iroquois transcription factors in kidney development. *Cell Dev Biol* 2014; **3**:1000131.
25. Alarcon P, Rodriguez-Seguel E, Fernandez-Gonzalez A, Rubio R, Gomez-Skarmeta JL. A dual requirement for Iroquois genes during Xenopus kidney development. *Development* 2008; **135**:3197–3207.
26. Krisher RL. The effect of oocyte quality on development. *J Anim Sci* 2004; **82 E-Suppl**:E14–E23.
27. Gilchrist RB, Lane M, Thompson JG. Oocyte-secreted factors: Regulators of cumulus cell function and oocyte quality. *Hum Reprod Update* 2008; **14**:159–177.
28. He W, Jia Y, Takimoto K. Interaction between transcription factors Iroquois proteins 4 and 5 controls cardiac potassium channel Kv4.2 gene transcription. *Cardiovasc Res* 2009; **81**:64–71.
29. Oktay K, Briggs D, Gosden RG. Ontogeny of follicle-stimulating hormone receptor gene expression in isolated human ovarian follicles. *J Clin Endocrinol Metab* 1997; **82**:3748–3751.
30. Cortvrindt R, Hu Y, Smitz J. Recombinant luteinizing hormone as a survival and differentiation factor increases oocyte maturation in recombinant follicle stimulating hormone-supplemented mouse preantral follicle culture. *Hum Reprod* 1998; **13**:1292–1302.
31. Richards JS, Ascoli M. Endocrine, paracrine, and Autocrine Signaling pathways that regulate ovulation. *Trends Endocrinol Metab* 2018; **29**:313–325.
32. Lei ZM, Mishra S, Zou W, Xu B, Foltz M, Li X, Rao CV. Targeted disruption of luteinizing hormone/human chorionic gonadotropin receptor gene. *Mol Endocrinol* 2001; **15**:184–200.
33. Rao CV, Lei ZM. Consequences of targeted inactivation of LH receptors. *Mol Cell Endocrinol* 2002; **187**:57–67.
34. Hsieh M, Thao K, Conti M. Genetic dissection of epidermal growth factor receptor signaling during luteinizing hormone-induced oocyte maturation. *PLoS One* 2011; **6**:e21574.
35. Sela-Abramovich S, Chorev E, Galiani D, Dekel N. Mitogen-activated protein kinase mediates luteinizing hormone-induced breakdown of communication and oocyte maturation in rat ovarian follicles. *Endocrinology* 2005; **146**:1236–1244.
36. Simon AM, Goodenough DA, Li E, Paul DL. Female infertility in mice lacking connexin 37. *Nature* 1997; **385**:525–529.
37. Norris RP, Freudzon M, Mehlmann LM, Cowan AE, Simon AM, Paul DL, Lampe PD, Jaffe LA. Luteinizing hormone causes MAP kinase-dependent phosphorylation and closure of connexin 43 gap junctions in mouse ovarian follicles: One of two paths to meiotic resumption. *Development* 2008; **135**:3229–3238.
38. Conti M, Hsieh M, Zamah AM, Oh JS. Novel signaling mechanisms in the ovary during oocyte maturation and ovulation. *Mol Cell Endocrinol* 2012; **356**:65–73.
39. Tamamura Y, Katsube K, Mera H, Itokazu M, Wakitani S. Irx3 and Bmp2 regulate mouse mesenchymal cell chondrogenic differentiation in both a Sox9-dependent and -independent manner. *J Cell Physiol* 2017; **232**:3317–3336.
40. Das S, Maizels ET, DeManno D, St Clair E, Adam SA, Hunzicker-Dunn M. A stimulatory role of cyclic adenosine 3′,5′-monophosphate in follicle-stimulating hormone-activated mitogen-activated protein kinase signaling pathway in rat ovarian granulosa cells. *Endocrinology* 1996; **137**:967–974.
41. Maizels ET, Cottom J, Jones JC, Hunzicker-Dunn M. Follicle stimulating hormone (FSH) activates the p38 mitogen-activated protein kinase pathway, inducing small heat shock protein phosphorylation and cell rounding in immature rat ovarian granulosa cells. *Endocrinology* 1998; **139**:3353–3356.
42. Fan HY, Liu Z, Shimada M, Sterneck E, Johnson PF, Hedrick SM, Richards JS. MAPK3/1 (ERK1/2) in ovarian granulosa cells are essential for female fertility. *Science* 2009; **324**:938–941.
43. Gaborit N, Varro A, Le Bouter S, Szuts V, Escande D, Nattel S, Demolombe S. Gender-related differences in ion-channel and transporter subunit expression in non-diseased human hearts. *J Mol Cell Cardiol* 2010; **49**:639–646.
44. Hara S, Kato T, Goto Y, Kubota S, Tamano M, Terao M, Takada S. Microinjection-based generation of mutant mice with a double mutation and a 0.5 Mb deletion in their genome by the CRISPR/Cas9 system. *J Reprod Dev* 2016; **62**:531–536.